ACS APPLIED MATERIALS & INTERFACES

Research Article

www.acsami.org

Randomly Distributed Conjugated Polymer Repeat Units for High-Efficiency Photovoltaic Materials with Enhanced Solubility and Processability

Bing Xu,[†] Ian Pelse,[†] Shruti Agarkar,[†] Shunichiro Ito,[†,‡] Junxiang Zhang,[†] Xueping Yi,[§] Yoshiki Chujo,[‡] Seth Marder,[∥] Franky So,[§] and John R. Reynolds*[,∥]

[†]School of Chemistry and Biochemistry, Center for Organic Photonics and Electronics, and [∥]School of Chemistry and Biochemistry and School of Materials Science and Engineering, Center for Organic Photonics and Electronics, Georgia Tech Polymer Network, Georgia Institute of Technology, Atlanta, Georgia 30332, United States

[‡]Department of Polymer Chemistry, Graduate School of Engineering, Kyoto University, Katsura, Nishikyo-ku, Kyoto 615-8510, Japan

[§]Department of Materials Science and Engineering, North Carolina State University, Raleigh, North Carolina 27606, United States

Supporting Information

ABSTRACT: Three structurally disordered terpolymer derivatives of PffBT4T-2OD (PCE11), prepared by replacing a varied amount of bithiophene linkers with single thiophenes, were found to exhibit reduced aggregation in solution with increasing thiophene content, while important redox and optoelectronic properties remained similar to those of PffBT4T-2OD. Solar cells based on random terpolymer-$PC_{71}BM$ blends exhibited average power conversion efficiencies of over 9.5% when processed with preheated substrates, with fill factors above 70%, exceeding those from PffBT4T-2OD. Thanks to increased solubility, random terpolymer devices were able to be fabricated on room-temperature substrates, reaching virtually identical performance among all three polymers despite remarkable thicknesses of ∼400 nm. Thus, we show that the random terpolymer approach is successful in improving processability while maintaining device performance.

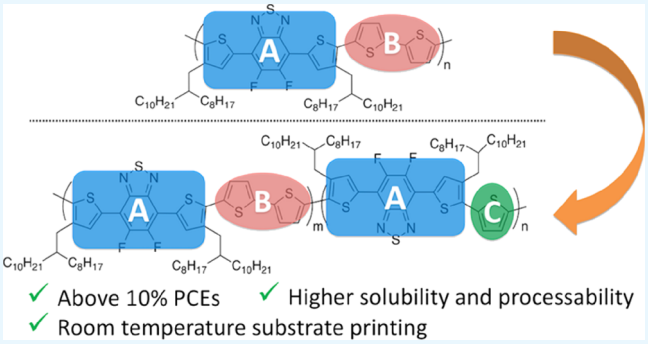

KEYWORDS: *conjugated polymers, organic photovoltaics, random terpolymers, bulk heterojunction solar cells, organic electronics*

Over the past decade, polymer-based organic photovoltaic (OPV) bulk heterojunction (BHJ) devices have advanced to the point that power conversion efficiencies (PCEs), now exceed 14% for single-junction cells.[1−5] The donor polymer PffBT4T-2OD [poly[(5,6-difluoro-2,1,3-benzothiadiazol-4,7-diyl)-*alt*-(3,3‴-di(2-octyldodecyl)-2,2′;5′,2″;5″,2‴-quaterthiophen-5,5-diyl)] (so called PCE11) has been reported to provide one of the highest PCEs in the field (>10% with multiple fullerene derivatives), and variants on it can be synthesized readily by varying the structure of the two monomers copolymerized to yield the active material.[6−9] A major challenge encountered when processing PCE11 is its observed strongly temperature-dependent aggregation, which can complicate the process of forming BHJ films with morphologies that lead to high PCEs. This has inspired studies aimed at either controlling the polymer molecular weight or modifying the polymer structure in order to enhance solubility and processability.[10−13]

Employing random polymerization in the preparation of well-performing donor−acceptor (DA) conjugated polymers as OPV materials has proven to be a practical and convenient approach for polymer structural modification. Using this approach, the resulting polymers can exhibit a broader absorption band across the visible and near IR region of the spectrum relative to a simple DA alternating polymer because of the presence of a variety of chromophores, which can lead to higher short-circuit current (J_{sc}) values in devices.[14−19] Further, random polymers may have higher solubility and a lower tendency to aggregate in comparison to parent polymers with more regular repeat units. In addition, the degree of crystallinity can be tuned based on polymer composition, thus allowing a modicum of control of the blend morphology in BHJ solar cells.[12,20−29] These physical aspects motivated our interest to introduce randomness into the backbone of PffBT4T-2OD as a means of improving polymer solubility and processability, while retaining straightforward monomer synthesis with only one side-chain functionalized unit.

Received: September 6, 2018
Accepted: November 29, 2018

DOI: 10.1021/acsami.8b15522
ACS Appl. Mater. Interfaces XXXX, XXX, XXX−XXX

Scheme 1. Structures of the Alternating and Random PCE11-Based Copolymers Studied in This Work

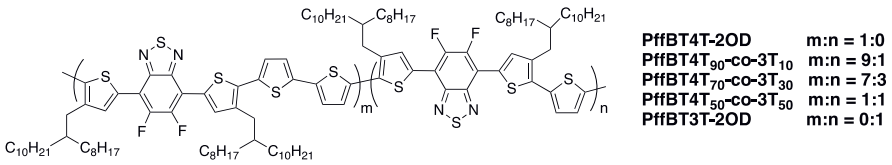

Here, we report our work on a set of random terpolymer derivatives of PffBT4T-2OD by replacing a fraction of the bithiophene linkers with single thiophenes, which led to a family of polymers with (1) a reduced tendency to aggregate and increased solubility of up to 50 mg/mL at room temperature, (2) facile monomer access similar to PffBT4T-2OD itself, (3) average PCEs approaching 10% in devices, exceeding those based on PffBT4T-2OD, and (4) less demanding processing requirements in device fabrication. Three random terpolymers with a varied bithiophene content were synthesized by Migita−Kosugi−Stille polymerization as shown in Schemes 1 and S1. The two alternating parent copolymers, PffBT4T-2OD and PffBT3T-2OD, were prepared as well for comparison. The polymer structures were verified by elemental analysis (see Supporting Information) and ^{1}H NMR spectroscopy. The peaks at δ 7.34 and 7.28 ppm in ^{1}H NMR spectra (Figures S1−S6) are characteristic of the aromatic protons on the mono- and bi-thiophenes, respectively, whose integrations were used to calculate the random terpolymer compositions. As summarized in Table S1, the calculated compositions of the synthesized terpolymers match their feed ratios with no more than 2 mol % deviation. As determined by high-temperature gel permeation chromatography at 140 °C in 1,2,4-trichlorobenzene, the polymers have similar-number average molecular weights (M_n) estimated to be ∼45 kDa with monomodal chromatograms, except for PffBT3T-2OD having a slightly higher M_n of 60.4 kDa (see Figure S7 in Supporting Information for chromatograms). This minimizes the possible influence of molecular weight differences on the polymer solubility, molecular packing, and blend morphology.[9]

The strong temperature dependence of PffBT4T-2OD to aggregate is manifested by its remarkable thermochromic behavior in dilute solution illustrated in Figures 1 and S8, where the maximum absorption wavelength (λ_{max}) shifts from ∼700 nm at 25 °C associated with the aggregated polymers to ∼550 nm at 85 °C, as aggregates break up to molecularly dissolved species.[6] A similar thermochromic behavior was observed for the other polymers as well, as shown in Figure S8. In general, the thermochromic behavior becomes less pronounced as the monothiophene content is increased at the expense of the bithiophene content in the polymers. This phenomenon can be easily visualized by the comparison of normalized UV−vis absorption profiles of the five polymer solutions at 25 °C, as shown in Figure 1a. As the thiophene content in the polymer increases, the absorption intensity at around 700 nm reduces; the peak at 700 nm disappears completely for PffBT4T$_{50}$-*co*-3T$_{50}$ and PffBT3T-2OD, with their λ_{max} found below 600 nm. This phenomenon is indicative of a reduction in aggregation of the polymer chains as the bithiophene linkers are replaced by single thiophenes. UV−vis absorption spectra of the annealed spin-coated thin films are shown in Figure 1b. All samples exhibit similar λ_{max} values around 700 nm and absorption peak shapes, suggesting that replacing the bithiophene units with thiophenes does not

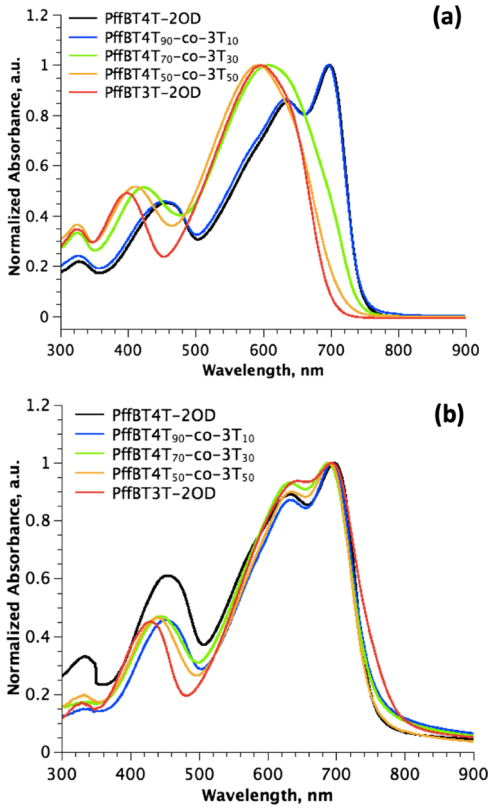

Figure 1. Normalized UV−vis absorption profiles of the polymers (a) in dilute *o*-dichlorobenzene solution (0.02 mg/mL) at 25 °C and (b) as spin-coated thin films annealed at 150 °C for 15 min.

significantly alter the polymer optoelectronic properties in the solid state. The absorption onset wavelength of PffBT3T-2OD is slightly longer than that of the other polymers, corresponding to a slightly lower optical gap (determined by the onset wavelength of UV−vis absorption profiles) of 1.59 eV, compared to 1.65 eV for all the other polymers.

As the aggregation in solution becomes weaker with a higher monothiophene content in the polymer, the solubility in typical organic solvents increases remarkably. For example, where PffBT4T-2OD does not effectively dissolve in chlorobenzene at room temperature, the polymers that have 30% monothiophene content and above can be processed from 6 mg/mL chlorobenzene solutions at room temperature to form uniform films. The room-temperature solubilities of both PffBT4T$_{50}$-*co*-3T$_{50}$ and PffBT3T-2OD in chlorobenzene are as high as 50 mg/mL. At the same time, the monothiophene content has a minimal effect of ∼50 mV on the onset of the differential pulse voltammetry (DPV) oxidation curves (see Figure S9 and Table S2 in Supporting Information), indicating that only a small change in the ionization energy is to be expected. In addition, hole mobilities of the alternating and random copolymers, measured by the space-charge limited current method, are all comparable in magnitude to that of

DOI: 10.1021/acsami.8b15522
ACS Appl. Mater. Interfaces XXXX, XXX, XXX−XXX

PffBT4T-2OD on the order of 10^{-3} cm^2/V s (see Table S2), which is consistent with the value reported in previous literature.[9]

Thermogravimetric analysis (TGA) of the random terpolymers and PffBT3T-2OD shows that each polymer has high thermal stability as no weight loss can be observed until ~350 °C, and temperatures above 400 °C are needed to achieve 5% weight loss of each sample (see Figure S10 in Supporting Information). Differential scanning calorimetry (DSC) was used to monitor the thermal properties of the polymers in the solid-state. Figure 2 shows the melting transitions of the

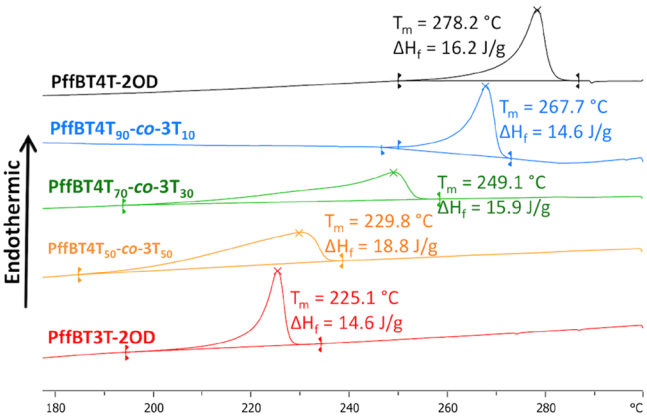

Figure 2. Second heating cycles of DSC curves of all five polymers. PffBT4T-2OD (T_m = 278.2 °C, ΔH_f = 16.2 J/g); PffBT4T$_{90}$-*co*-3T$_{10}$ (T_m = 267.7 °C, ΔH_f = 14.6 J/g); PffBT4T$_{70}$-*co*-3T$_{30}$ (T_m = 249.1 °C, ΔH_f = 15.9 J/g); PffBT4T$_{50}$-*co*-3T$_{50}$ (T_m = 229.8 °C, ΔH_f = 18.8 J/g); PffBT3T-2OD (T_m = 225.1 °C, ΔH_f = 14.6 J/g).

second heating/cooling cycles for each polymer. The melt-transition temperatures (T_m) of the random terpolymers fall in between those of the two alternating copolymers, PffBT4T-2OD and PffBT3T-2OD, and follow a trend that the transition temperatures decrease as more monothiophene repeat units are present in the terpolymer backbones. Similar phenomena can be seen for the crystallization temperatures (T_c) as well in Figure S11, where the full curves for the second heating/cooling cycles are shown. Such changes in T_m and T_c are in agreement with previous reports on random conjugated terpolymers,[12,27,29] and are highlighted in Figure 3, where the relationship of T_m and T_c to the monothiophene content is shown. In addition, compared to the alternating copolymers, the random terpolymers show a broader temperature range for both melting and crystallization transitions, which is a typical behavior for random copolymers.[30] The heat of fusion (ΔH_f) and heat of crystallization (ΔH_c) for all polymers were calculated and can be seen in Figures 2 and S11. Interestingly, the values are found to be quite similar between 14 and 19 J/g independent of the copolymer composition, in contrast to the previous findings that particular random terpolymers had lower melting enthalpies than the parent alternating copolymers.[29] This suggests that the random terpolymer derivatives of PffBT4T-2OD and PffBT3T-2OD do not necessarily have less crystallinity in the solid state, although their aggregation in solution is suppressed compared to PffBT4T-2OD. This observation is similar to what was previously reported for another random PffBT4T-2OD system,[12] where the DSC curves of all five random copolymers showed strong tendency to form highly crystalline domains.

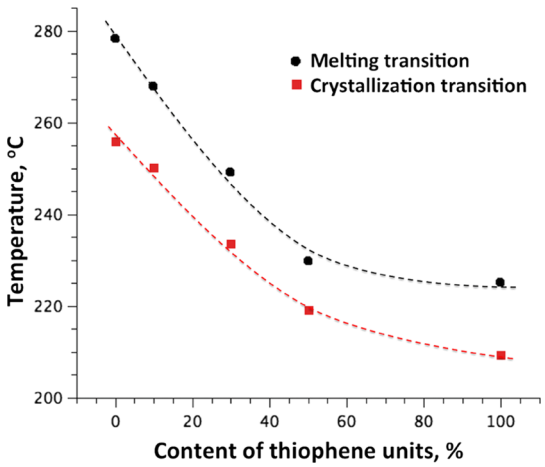

Figure 3. Temperatures of melting and crystallization transitions (peak values) vs polymer backbone compositions (the content of thiophene units). Dashed lines are to guide the eyes.

The performance of the DA copolymers and terpolymers as donor-phase materials in BHJ solar cells were investigated with $PC_{71}BM$ as the electron acceptor-phase material. Devices were fabricated by preheating both the blend solution and indium tin oxide (ITO) substrate at 110 °C and by using a custom fabricated chuck for the spin coater with elevated edges to prevent heat dissipation from the hot substrate, which was optimized for processing PffBT4T-2OD (experimental details available in Supporting Information). The average device parameters are summarized in Table 1, and the current density−voltage (J−V) characteristics of the best performing devices are shown in Figure S12. We find the three random terpolymers to exhibit average PCEs over 9%, exceeding those based on either of the two alternating copolymers. Such an enhancement in PCE is mostly owing to the high fill factors (FFs) above 70%, while the J_{sc} and open circuit voltage (V_{oc}) values remain similar to those based on PffBT4T-2OD. The external quantum efficiency (EQE) results shown in Figure S13 in Supporting Information have verified the J_{sc} values achieved from J−V curves, with discrepancies within 10%, as shown in Table S3. In particular, the random terpolymers have led to high incident photon to current conversion efficiencies approaching 80% from 370 to 730 nm.

Grazing-incidence wide-angle X-ray scattering (GIWAXS) images of the pristine polymers are shown in Figure S14 in Supporting Information, and those of the blends are shown in Figures 4a,b and S15. For these measurements, hot solutions at 110 °C were spin-coated onto silicon substrates that were roughly 75 °C. The one-dimensional (1D) line-cuts in the in-plane and out-of-plane directions for all blend samples can be seen in Figures 4c and S16, respectively. Overall, the morphology among all polymers is very similar. In the two-dimensional (2D) images of the blends (see Figures 4 and S15), both lamellar packing and π−π stacking signals can be observed for all five samples, suggesting that each of these copolymers exhibit semicrystalline features in the blends with $PC_{71}BM$ despite their varied tendency to aggregate in solution. The diffraction signal associated with π−π stacking of the polymer backbone appears in the out-of-plane direction, indicating that each of the polymers mainly adopts a face-on orientation relative to the substrate. This is consistent with previous reports of PffBT4T-2OD deposited via blade coating at slightly cooler temperatures than the optimum substrate

DOI: 10.1021/acsami.8b15522
ACS Appl. Mater. Interfaces XXXX, XXX, XXX−XXX

Table 1. Summary of Average Device Characteristics for Solar Cells

polymer/$PC_{71}BM$	substrate temperature[a]	J_{sc} (mA/cm^2)	V_{oc} (V)	FF (%)	PCE (%)
PffBT4T-2OD	preheated	18.2 ± 1.2	0.70 ± 0.01	69 ± 2	8.7 ± 0.6
PffBT4T^{90}-*co*-3T$_{10}$	preheated	18.5 ± 0.6	0.72 ± 0.01	73 ± 1	9.6 ± 0.6
PffBT4T$_{70}$-*co*-3T$_{30}$	preheated	17.7 ± 1.0	0.73 ± 0.01	74 ± 1	9.6 ± 0.6
PffBT4T$_{50}$-*co*-3T$_{50}$	preheated	17.6 ± 0.8	0.72 ± 0.01	72 ± 1	9.1 ± 0.6
PffBT3T-2OD	preheated	12.0 ± 0.4	0.74 ± 0.01	69 ± 2	5.1 ± 0.7
PffBT4T$_{90}$-*co*-3T$_{10}$	rt	19.9 ± 0.8	0.73 ± 0.01	65 ± 4	9.6 ± 0.5
PffBT4T$_{70}$-*co*-3T$_{30}$	rt	17.5 ± 0.5	0.75 ± 0.01	72 ± 1	9.5 ± 0.3
PffBT4T$_{50}$-*co*-3T$_{50}$	rt	16.6 ± 1.2	0.74 ± 0.01	74 ± 1	9.1 ± 0.6
PffBT3T-2OD	rt	14.0 ± 0.4	0.74 ± 0.01	58 ± 5	6.0 ± 0.9

[a]For processing with preheated substrates, prior to spin coating, both the blend solution and ITO substrates were preheated on a hot plate at 110 °C; a custom fabricated chuck for the spin coater with elevated edges was used to prevent heat dissipation from the hot substrate to the spin coater to ensure good coverage of the solution. For processing with rt substrates, the substrates were kept at room temperature using a regular substrate holder instead of the custom chuck with elevated edges, and the solution was heated at 90 °C for 2 h. Experimental details can be found in the Supporting Information.

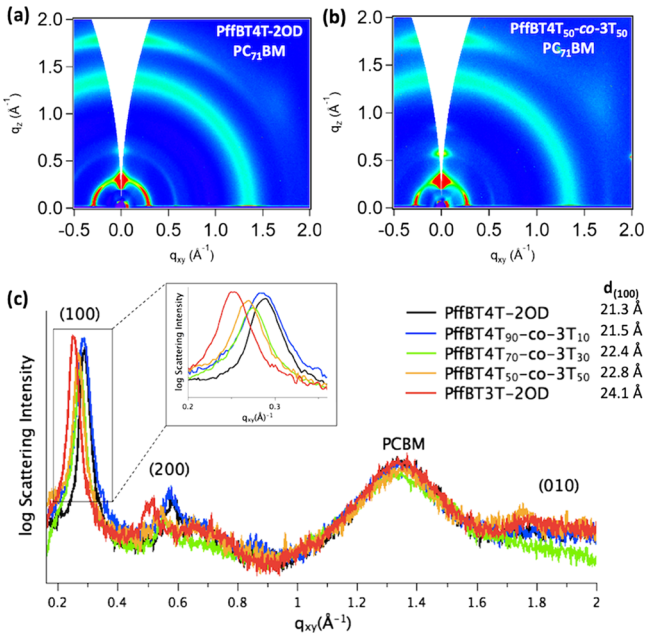

Figure 4. 2D GIWAXS patterns of (a) PffBT4T-2OD:$PC_{71}BM$ blends, (b) PffBT4T$_{50}$-*co*-3T$_{50}$:$PC_{71}BM$ blends, and (c) 1D line-cut profiles in in-plane direction (right images).

temperature of 110 °C.[7] The signals corresponding to the lamellar packing are present in both in-plane and out-of-plane directions, which suggests that there is a certain degree of isotropic distribution of the packed polymer chain orientations. Such observations are also seen in the GIWAXS results of the pristine polymer films, as shown in Figure S14 in Supporting Information.

Minimal yet observable differences can be found in the in-plane lamellar packing distances, which are annotated for each polymer/$PC_{71}BM$ film as $d_{(100)}$ in Figure 4c. As the monothiophene linkers are introduced into the polymer backbones, the *d*-spacings attributed to lamellar packing gradually increase from 21.3 nm for PffBT4T-2OD to 24.1 nm for PffBT3T-2OD. This can be attributed to the closer proximity between the solubilizing side chains along the polymer backbone when thiophene linkers are present, interrupting the interdigitation of side chains. A higher volume percentage of side chain may additionally induce order and could explain why the backbones are driven farther apart.

As the random terpolymers and PffBT3T-2OD are more soluble and have less of a tendency to aggregate in solution relative to PffBT4T-2OD, we surmised they might be easier to process than the parent PffBT4T-2OD. To test this hypothesis, devices were prepared with warm processing solutions (90 °C) deposited on room-temperature substrates (experimental details available in Supporting Information) and the results are presented in Figure S17 and Table 1. Because of the strong aggregation of PffBT4T-2OD, its blend with $PC_{71}BM$ becomes a gel immediately after being transferred onto the room-temperature substrate (illustrated by the photograph in Figure S18), preventing it from forming a uniform film and subsequently making a functional device. In sharp contrast, all random terpolymers lead to devices that perform similar to their hot-substrate processed counterparts. Generally, when building devices on room-temperature substrates, current increases while FF decreases, which is an indication of a thicker active layer film being formed. Indeed, film thicknesses for the three random terpolymer active layers increased from ∼250 to ∼400 nm as we moved from heated to room-temperature substrates (see Table S4), the latter of which is significantly thicker than active layers typically found in OPV devices. These results confirm that the random terpolymer approach is successful in improving the solubility and processability of conjugated polymers, which can provide practical implications in ease of device fabrication.

In summary, we have demonstrated that random terpolymers based on the PffBT4T-2OD parent copolymer with varied amounts of monothiophene linkers replacing bithiophene had reduced aggregation in solution with an increasing monothiophene content, and due to the favorable blend morphology and high hole mobility on the order of 10^{-3} cm^2/V s, the resulting fullerene-based solar cells could reach PCEs averaging above 9.5% with especially high FFs of over 70%. Importantly, as the polymers aggregated less and exhibited higher solubility at room temperature, devices based on the random terpolymers could be prepared on room-temperature substrates and achieve a very similar performance, even at remarkably thick films of ∼400 nm. This latter point is especially important as one considers the future of coating and printing organic solar cells where the use of room-temperature substrates will make practical processing more facile.

DOI: 10.1021/acsami.8b15522
ACS Appl. Mater. Interfaces XXXX, XXX, XXX−XXX

■ ASSOCIATED CONTENT

Supporting Information

The Supporting Information is available free of charge on the ACS Publications website at DOI: 10.1021/acsami.8b15522.

Experimental details including materials, polymer syntheses, characterization methods, and device fabrication and measurements, ^{1}H spectra of synthesized polymers, polymerization result summary, UV−vis absorption profiles, cyclic voltammetry, and DPV curves, TGA and DSC heating and cooling curves, summary of the polymer optoelectronic, thermal and redox properties and hole mobilities, *J*−*V* and EQE characteristics of devices, short circuit current density from devices built on preheated substrates as measured from the solar data and integrated from the EQE data, 2D GIWAXS figures for pristine polymers and polymer/$PC_{71}BM$ blends, GIWAXS 1D line-cuts in the out-of-plane direction for polymer/$PC_{71}BM$ blends, device active layer film thicknesses, photo of the PffBT4T-2OD:$PC_{71}BM$ blend spin-coated on room-temperature substrate (PDF)

■ AUTHOR INFORMATION

Corresponding Author

*E-mail: reynolds@chemistry.gatech.edu.

ORCID

Bing Xu: 0000-0001-7138-8936
Seth Marder: 0000-0001-6921-2536
Franky So: 0000-0002-8310-677X
John R. Reynolds: 0000-0002-7417-4869

Author Contributions

The manuscript was written through contributions of all authors. All authors have given approval to the final version of the manuscript.

Notes

The authors declare no competing financial interest.

■ ACKNOWLEDGMENTS

This work was supported by the Department of the Navy, Office of Naval Research Multidisciplinary University Research Initiative award no. N00014-16-1-2520 (S.M. and J.R.R.) and grants N00014-17-1-2243 (J.R.R.) and N00014-17-1-2242 (F.S.). Use of the Stanford Synchrotron Radiation Lightsource, SLAC National Accelerator Laboratory, is supported by the U.S. Department of Energy, Office of Science, Office of Basic Energy Sciences, under contract no. DE-AC02-76SF00515. I.P. was supported by the Department of Defense (DoD) through the National Defense Science & Engineering Graduate Fellowship (NDSEG) Program. S.M. and J.Z. acknowledge the support by the NSF under the CCI Center for Selective C−H Functionalization, CHE-1700982.

■ REFERENCES

(1) Zhao, W.; Li, S.; Yao, H.; Zhang, S.; Zhang, Y.; Yang, B.; Hou, J. Molecular Optimization Enables over 13% Efficiency in Organic Solar Cells. *J. Am. Chem. Soc.* **2017**, *139*, 7148−7151.

(2) Zhao, F.; Dai, S.; Wu, Y.; Zhang, Q.; Wang, J.; Jiang, L.; Ling, Q.; Wei, Z.; Ma, W.; You, W.; Wang, C.; Zhan, X. Single-Junction Binary-Blend Nonfullerene Polymer Solar Cells with 12.1% Efficiency. *Adv. Mater.* **2017**, *29*, 1700144.

(3) Luo, Z.; Bin, H.; Liu, T.; Zhang, Z.-G.; Yang, Y.; Zhong, C.; Qiu, B.; Li, G.; Gao, W.; Xie, D.; Wu, K.; Sun, Y.; Liu, F.; Li, Y.; Yang, C. Fine-Tuning of Molecular Packing and Energy Level through Methyl Substitution Enabling Excellent Small Molecule Acceptors for Nonfullerene Polymer Solar Cells with Efficiency up to 12.54%. *Adv. Mater.* **2018**, *30*, 1706124.

(4) Zhang, S.; Qin, Y.; Zhu, J.; Hou, J. Over 14% Efficiency in Polymer Solar Cells Enabled by a Chlorinated Polymer Donor. *Adv. Mater.* **2018**, *30*, 1800868.

(5) Li, S.; Ye, L.; Zhao, W.; Yan, H.; Yang, B.; Liu, D.; Li, W.; Ade, H.; Hou, J. A Wide Band Gap Polymer with a Deep Highest Occupied Molecular Orbital Level Enables 14.2% Efficiency in Polymer Solar Cells. *J. Am. Chem. Soc.* **2018**, *140*, 7159−7167.

(6) Liu, Y.; Zhao, J.; Li, Z.; Mu, C.; Ma, W.; Hu, H.; Jiang, K.; Lin, H.; Ade, H.; Yan, H. Aggregation and Morphology Control Enables Multiple Cases of High-Efficiency Polymer Solar Cells. *Nat. Commun.* **2014**, *5*, 5293.

(7) Ro, H. W.; Downing, J. M.; Engmann, S.; Herzing, A. A.; DeLongchamp, D. M.; Richter, L. J.; Mukherjee, S.; Ade, H.; Abdelsamie, M.; Jagadamma, L. K.; Amassian, A.; Liu, Y.; Yan, H. Morphology Changes upon Scaling a High-Efficiency, Solution-Processed Solar Cell. *Energy Environ. Sci.* **2016**, *9*, 2835−2846.

(8) Hu, H.; Chow, P. C. Y.; Zhang, G.; Ma, T.; Liu, J.; Yang, G.; Yan, H. Design of Donor Polymers with Strong Temperature-Dependent Aggregation Property for Efficient Organic Photovoltaics. *Acc. Chem. Res.* **2017**, *50*, 2519−2528.

(9) Ma, W.; Yang, G.; Jiang, K.; Carpenter, J. H.; Wu, Y.; Meng, X.; McAfee, T.; Zhao, J.; Zhu, C.; Wang, C.; Ade, H.; Yan, H. Influence of Processing Parameters and Molecular Weight on the Morphology and Properties of High-Performance PffBT4T-2OD:PC71BM Organic Solar Cells. *Adv. Energy Mater.* **2015**, *5*, 1501400.

(10) Pirotte, G.; Agarkar, S.; Xu, B.; Zhang, J.; Lutsen, L.; Vanderzande, D.; Yan, H.; Pollet, P.; Reynolds, J. R.; Maes, W.; Marder, S. R. Molecular Weight Tuning of Low Bandgap Polymers by Continuous Flow Chemistry: Increasing the Applicability of PffBT4T for Organic Photovoltaics. *J. Mater. Chem. A* **2017**, *5*, 18166−18175.

(11) Zhao, J.; Li, Y.; Lin, H.; Liu, Y.; Jiang, K.; Mu, C.; Ma, T.; Lin Lai, J. Y.; Hu, H.; Yu, D.; Yan, H. High-efficiency Non-Fullerene Organic Solar Cells Enabled by a Difluorobenzothiadiazole-Based Donor Polymer Combined with a Properly Matched Small Molecule Acceptor. *Energy Environ. Sci.* **2015**, *8*, 520−525.

(12) Yao, H.; Li, Y.; Hu, H.; Chow, P. C. Y.; Chen, S.; Zhao, J.; Li, Z.; Carpenter, J. H.; Lai, J. Y. L.; Yang, G.; Liu, Y.; Lin, H.; Ade, H.; Yan, H. A Facile Method to Fine-Tune Polymer Aggregation Properties and Blend Morphology of Polymer Solar Cells Using Donor Polymers with Randomly Distributed Alkyl Chains. *Adv. Energy Mater.* **2017**, *8*, 1701895.

(13) Li, M.; An, C.; Marszalek, T.; Baumgarten, M.; Yan, H.; Müllen, K.; Pisula, W. Controlling the Surface Organization of Conjugated Donor-Acceptor Polymers by their Aggregation in Solution. *Adv. Mater.* **2016**, *28*, 9430−9438.

(14) Beaupré, S.; Shaker-Sepasgozar, S.; Najari, A.; Leclerc, M. Random D-A1-D-A2 Terpolymers Based on Benzodithiophene, Thiadiazole[3,4-e]isoindole-5,7-dione and Thieno[3,4-c]pyrrole-4,6-dione for Efficient Polymer Solar Cells. *J. Mater. Chem. A* **2017**, *5*, 6638−6647.

(15) Jung, J. W.; Liu, F.; Russell, T. P.; Jo, W. H. Semi-Crystalline Random Conjugated Copolymers with Panchromatic Absorption for Highly Efficient Polymer Solar Cells. *Energy Environ. Sci.* **2013**, *6*, 3301−3307.

(16) Kang, T. E.; Cho, H.-H.; Kim, H. j.; Lee, W.; Kang, H.; Kim, B. J. Importance of Optimal Composition in Random Terpolymer-Based Polymer Solar Cells. *Macromolecules* **2013**, *46*, 6806−6813.

(17) Kang, T. E.; Choi, J.; Cho, H.-H.; Yoon, S. C.; Kim, B. J. Donor-Acceptor Random versus Alternating Copolymers for Efficient Polymer Solar Cells: Importance of Optimal Composition in Random Copolymers. *Macromolecules* **2016**, *49*, 2096−2105.

(18) Lee, J. W.; Ahn, H.; Jo, W. H. Conjugated Random Copolymers Consisting of Pyridine- and Thiophene-Capped

DOI: 10.1021/acsami.8b15522
ACS Appl. Mater. Interfaces XXXX, XXX, XXX−XXX

Diketopyrrolopyrrole as Co-Electron Accepting Units To Enhance both JSC and VOC of Polymer Solar Cells. *Macromolecules* **2015**, *48*, 7836−7842.

(19) Zhu, X.; Lu, K.; Xia, B.; Fang, J.; Zhao, Y.; Zhao, T.; Wei, Z.; Jiang, L. Improving the Performances of Random Copolymer Based Organic Solar Cells by Adjusting the Film Features of Active Layers Using Mixed Solvents. *Polymers* **2016**, *8*, 4.

(20) Chen, S.; Cho, H. J.; Lee, J.; Yang, Y.; Zhang, Z.-G.; Li, Y.; Yang, C. Modulating the Molecular Packing and Nanophase Blending via a Random Terpolymerization Strategy toward 11% Efficiency Nonfullerene Polymer Solar Cells. *Adv. Energy Mater.* **2017**, *7*, 1701125.

(21) Cho, H. J.; Kim, Y. J.; Chen, S.; Lee, J.; Shin, T. J.; Park, C. E.; Yang, C. Over 10% Efficiency in Single-Junction Polymer Solar Cells Developed from Easily Accessible Random Terpolymers. *Nano Energy* **2017**, *39*, 229−237.

(22) Duan, C.; Gao, K.; van Franeker, J. J.; Liu, F.; Wienk, M. M.; Janssen, R. A. J. Toward Practical Useful Polymers for Highly Efficient Solar Cells via a Random Copolymer Approach. *J. Am. Chem. Soc.* **2016**, *138*, 10782−10785.

(23) Gross, Y. M.; Trefz, D.; Tkachov, R.; Untilova, V.; Brinkmann, M.; Schulz, G. L.; Ludwigs, S. Tuning Aggregation by Regioregularity for High-Performance n-Type P(NDI2OD-T2) Donor-Acceptor Copolymers. *Macromolecules* **2017**, *50*, 5353−5366.

(24) Hwang, Y.-J.; Earmme, T.; Courtright, B. A. E.; Eberle, F. N.; Jenekhe, S. A. n-Type Semiconducting Naphthalene Diimide-Perylene Diimide Copolymers: Controlling Crystallinity, Blend Morphology, and Compatibility Toward High-Performance All-Polymer Solar Cells. *J. Am. Chem. Soc.* **2015**, *137*, 4424−4434.

(25) Jeong, M.; Chen, S.; Lee, S. M.; Wang, Z.; Yang, Y.; Zhang, Z.-G.; Zhang, C.; Xiao, M.; Li, Y.; Yang, C. Feasible D1-A-D2-A Random Copolymers for Simultaneous High-Performance Fullerene and Nonfullerene Solar Cells. *Adv. Energy Mater.* **2017**, *8*, 1702166.

(26) Kang, T. E.; Kim, K.-H.; Kim, B. J. Design of Terpolymers as Electron Donors for Highly Efficient Polymer Solar Cells. *J. Mater. Chem. A* **2014**, *2*, 15252−15267.

(27) Kim, K.-H.; Park, S.; Yu, H.; Kang, H.; Song, I.; Oh, J. H.; Kim, B. J. Determining Optimal Crystallinity of Diketopyrrolopyrrole-Based Terpolymers for Highly Efficient Polymer Solar Cells and Transistors. *Chem. Mater.* **2014**, *26*, 6963−6970.

(28) Wang, Q.; Wang, Y.; Zheng, W.; Shahid, B.; Qiu, M.; Wang, D.; Zhu, D.; Yang, R. Regulating Molecular Aggregations of Polymers via Ternary Copolymerization Strategy for Efficient Solar Cells. *ACS Appl. Mater. Interfaces* **2017**, *9*, 32126−32134.

(29) Li, Z.; Xu, X.; Zhang, W.; Meng, X.; Ma, W.; Yartsev, A.; Inganäs, O.; Andersson, M. R.; Janssen, R. A. J.; Wang, E. High Performance All-Polymer Solar Cells by Synergistic Effects of Fine-Tuned Crystallinity and Solvent Annealing. *J. Am. Chem. Soc.* **2016**, *138*, 10935−10944.

(30) Sanchez, I. C.; Eby, R. K. Crystallization of Random Copolymers. *J. Res. Natl. Bur. Stand., Sect. A* **1973**, *77*, 353−358.

DOI: 10.1021/acsami.8b15522
ACS Appl. Mater. Interfaces XXXX, XXX, XXX−XXX